Enhancing CAD-based shape optimization by automatically updating the CAD model's parameterization

Enhancing CAD-based shape optimization by automatically updating the CAD model's parameterization

Dheeraj Agarwal[1,3], Trevor T. Robinson[1]*, Cecil G. Armstrong[1], Christos Kapellos[2]

[1]School of Mechanical and Aerospace Engineering, Queen's University Belfast, Belfast BT9 5AH, Northern Ireland, UK
[2]Volkswagen AG, Group Research, CAE Methods, Wolfsburg Germany
[3]School of Mechanical and Maritime Engineering, Liverpool John Moores University, Liverpool, UK
*Email: t.robinson@qub.ac.uk

Abstract

This paper presents an approach which increases the flexibility of a computer-aided design (CAD) model by automatically refining its parameterization and adding new CAD features to the model´s feature tree. It aims to overcome the limitations imposed by the choice of parameters used during the initial model creation, which constrains how the model shape can change during design optimization. Parametric Effectiveness compares the maximum performance improvement that can be achieved using a parameterization strategy, to the maximum performance improvement that can be obtained where the model is unconstrained in how it moves. As such, it provides a measure of how good a parameterization strategy is and allows different strategies to be compared. The change in parametric effectiveness due to inserting multiple different CAD features can be calculated using a single adjoint analysis, therefore the computational cost is essentially independent of the number of parameterisation strategies being analysed. The described approach can be used to automatically add new features to the model, and subsequently allows the use of the newly-added parameters, along with the existing parameters to be used for optimization, providing the opportunity for a better performing product. The developed approach is applied on CAD models created in CATIA V5 for 2D and 3D finite element and computational fluid dynamics problems.

Keywords: CAD, feature, optimization, adjoint, parameterization

1. Introduction

Parametrization is at the core of optimization as it defines the design space the optimizing algorithm explores. The success of any shape optimization methodology depends extensively on the type of parameterization technique employed [1]. One straightforward route, which gives the most flexible parametrization strategy, is to use the nodes of the computational mesh [2-5] as design variables. One major drawback for this parameterization strategy is that, as all surface mesh nodes can move independently, the implementation of a post optimization smoothing algorithm is required to prevent the appearance of non-smooth shapes during the optimization process. In this regards, the Free-form deformation techniques have been successfully implemented for aerodynamic shape optimization problems [6-8]. These techniques originated from the soft object animation in the computer graphics industry [9]. The benefit of this approach is that it imparts smooth deformations to the analysis mesh and enables the parameterization to alter the thickness, sweep, twist, etc. for the design of an aerospace system. One of the drawbacks of these mesh-based optimization methods is that the mesh topology (in terms of the number of elements present and their connectivity) must remain constant as the model updates. Also, it is the mesh that reaches the optimum shape. As most manufacturing processes require a CAD model, this mesh must then be translated into a CAD model before it can be used for further analysis or manufacturing assessments. This mesh-to-CAD step is non-trivial and may require extensive user interaction [10, 11]. It is also very difficult to match the shape directly.

Using CAD geometry within the optimization process directly removes a lot of these difficult steps and should result in a better-quality model at the end of the process. It also aligns with the industrial ambition of having a more integrated design process. In a feature-based CAD modelling system (e.g. CATIA V5 [12]), a part model is comprised of individual features which are combined to represent an overall shape (see Fig. 1). In the context of CAD modelling, features can be defined in many ways depending on their application [13-15]. In this work, a feature is any operator in the CAD model feature tree that can be manipulated to change the model's shape, and a parameter is the dimensions associated with the feature. For example, these might control the shape of the sketches on which sketch based features (e.g. loft) are constructed, or the length of the feature (e.g. an extruded boss).

When creating a CAD model within a CAD modelling system, it is common to create relationships to specify that the value of one parameter is a function of the values of other parameters in the model. This relationship is part of the design intent of the model, and once applied the parameters they relate to cannot be controlled independently. The parameters which are responsible for changing the model's shape can have real, integer and Boolean values. These parameters can be accessed using a suitable CAD system application programming interface (API). In this paper, only continuous dimensional parameters which affect the shape of the model are considered. Modifying parameters with real values (such as lengths and angles) by small amounts will typically cause movements of the boundary proportional to, and of the same order as, the size of the parameter perturbation. In CATIA V5 the CAD features are stored in a feature tree as shown in Fig. 1(a) and a list of all of the parameters used to construct the model can be found through the "Formulas" window as seen in Fig. 1(b).

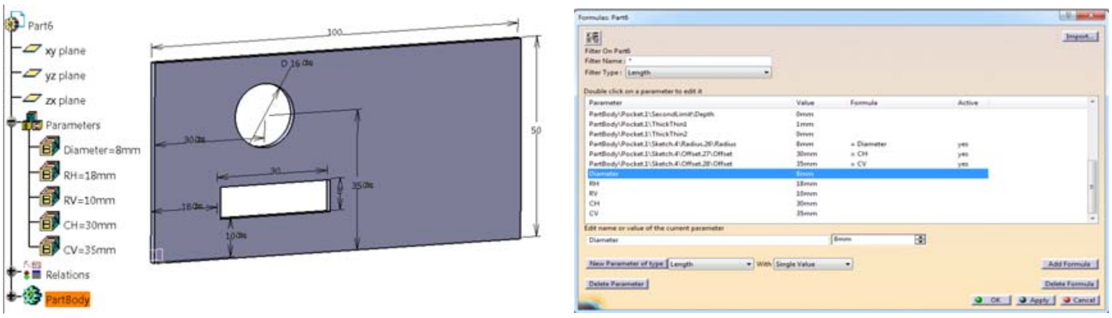

Double click on a parameter to edit it

Parameter	Value	Formula	Active
PartBody\Pocket.1\SecondLimit\Depth	0mm		
PartBody\Pocket.1\ThickThin1	1mm		
PartBody\Pocket.1\ThickThin2	0mm		
PartBody\Pocket.1\Sketch.4\Radius.26\Radius	8mm	= Diameter	yes
PartBody\Pocket.1\Sketch.4\Offset.27\Offset	30mm	= CH	yes
PartBody\Pocket.1\Sketch.4\Offset.28\Offset	35mm	= CV	yes
Diameter	8mm		
RH	18mm		
RV	10mm		
CH	30mm		
CV	35mm		

Edit name or value of the current parameter

Diameter 8mm

(a) (b)

Fig. 1 CATIA V5 feature tree representation

Some authors [16-20] have attempted to develop a link between optimization processes and CAD models through the use of non-uniform rational B-splines (NURBS) patches. A NURBS patch can be modified by moving its control points in all the directions and these can be used as optimization variables. Here the benefit is that the NURBS can represent a wide variety of shapes and represents a richer design space than that can be expressed using parameters in a feature-based CAD model. However, one downside of using NURBS is that sometimes the NURBS control net may be too coarse in certain regions and requires a process to enrich the control net by adding more control points before it is used for optimization. Jesudasan et al. [21] presented an adaptive parameterization approach based on NURBS patches, where the NURBS control net was refined by using knot insertion, and subsequently used to optimize pressure loss across a U-Bend passage of a turbine blade serpentine cooling passage. The downside of the approaches outlined above is that, as they do not work directly on the parametric CAD model created in a feature-based CAD system, the design intent and the parametric associativity captured in the choice of features used to build the model is lost.

If there is a desire to use CAD model parameters as variables for optimization, one of the key issues is that there is no clear link between the CAD parameters and the effect they have on performance, although Robinson et. al. [22] have shown an approach based on adjoint sensitivities which enables this. However, the ability to optimize the model is limited by the choice of CAD features in the model, and sometimes the parameters used to define these features may not be the best choice for optimization (in many instances they are not selected with optimization in mind). In this case, it is necessary either to re-parameterise the existing features (i.e. use a different way to control shape) or add more features (each with its own set of parameters) to increase the flexibility of the model. This is not straightforward especially if the person implementing these modifications is not the initial creator of the CAD model and is not fully aware of how it was constructed.

The adjoint surface sensitivities represent the derivative of the objective function with respect to the normal displacement of the surface mesh nodes. As such, the distribution of adjoint sensitivity over the surface of the model indicates how the boundary of the model should move to achieve an optimum improvement in performance. The advantage of the adjoint method arises from the fact that the gradient computation is independent of the number of design variables and so in the context of this work many parameterization strategies can be evaluated cheaply. The adjoint is computed by solving a problem of computational cost comparable to that of the primal analysis. A detailed description of the adjoint based approach can be found in [23-26]. The adjoint surface sensitivities can be integrated within a CAD-based optimization framework by calculating the parametric design velocity, i.e. the boundary shape movement resulting from a change in CAD parameter.

Parametric effectiveness [27] rates the ability of the parameters in a model to change its shape in the optimum way. Here, the optimum shape change is assumed to be that suggested by an adjoint sensitivity map on the model boundary. It ranges from 0 to 1. A low parametric effectiveness indicates that the parameters in the model are not able to perturb the CAD model shape in the manner the adjoint sensitivity map suggests. In this work, this is taken as an indication that it is better to reparametrize or add new features to the model before optimization. In [28], work was done to define the basic strategies for calculating the change in performance which could be achieved by the addition of small structural features including stiffener, boss, hole and pocket etc. But the authors did not detail how this could be used to automate the process as part of a general design strategy.

In this work, a framework is presented which increases the design flexibility of a CAD model automatically (by adding new features to the CAD model) when the parametric effectiveness is shown to be low. Thereafter, the full set of CAD parameters (new and original) are used to change the shape of the model. In this work this is achieved by updating the CAD model in two ways: (1) the sketch entities are modified – specifically straight lines are converted to splines and splines have additional control points added, and (2) by adding new sketch profiles to the definition of multi-section solid features that are common in both aerospace and automotive designs. The insertion of new features is done directly into the CAD model feature tree, so the model can be easily used for down-stream applications like manufacturing or process planning without any additional post-processing relative to a standard model. It will be argued here that the design decision on which CAD feature to insert, and where, can be made by analysing the adjoint sensitivities. Further, a comparison of parametric effectiveness and the optimization results for a number of CAD models is presented where different updating strategies are applied.

In this work, the CAD models are created in CATIA V5 and optimized using Sequential least square programming (SLSQP) method implemented in Scipy [29]. SLSQP is a gradient based optimization algorithm which minimizes a function with any combination of bounds, equality and inequality constraints. The advantage of using this algorithm is that it avoids the need for determining the weighting factors by including constraints directly into the optimization problem. Automated CAD system APIs are developed for refining the CAD features in Python 3.5 [30], and an interface with CATIA V5 is created using win32com object programming [31].

The remainder of the paper will first summarize the integration of the adjoint based sensitivity calculation with the design velocity. Section 3 presents the methodologies proposed for refining the CAD features and also inserting new features into the CAD model feature tree; the developments are demonstrated for the optimization of a loaded cantilever beam in section 4 and an automotive duct in section 5; the proposed methodology and the results are discussed in section 6; and the paper finishes with the main conclusions.

2. Theory

2.1. Design velocity

A key requirement when using CAD models for optimisation is the understanding of how the parameters defining the CAD model effect its shape. This is not always obvious from the CAD model feature tree, where the choice of modelling strategy is highly dependent on the preferences of the person who created the model. Design velocity (V_n) is the normal component of the displacement of the boundary of a CAD model. This work is concerned with computing the design velocity caused by the perturbations of the CAD parameters and is computed as

$$V_n = \delta X_s \cdot \hat{n}, \tag{1}$$

where δX_s is the movement of surface at a point on the boundary and $\hat{n}$ is the outward unit normal of the surface at that point. Now, considering the CAD model in Fig. 1, the parameters controlling the diameter of the hole and horizontal position of the slot are perturbed, and the design velocities are computed to represent the movement of the boundary in response, as shown in Fig. 2. The convention adopted throughout this work is that a positive design velocity represents an outward movement of the boundary, and negative is inward. Therefore, the hole diameter and right edge of the slot exhibit a negative design velocity in Fig. 2, whereas the design velocity at the left edge of the slot is positive.

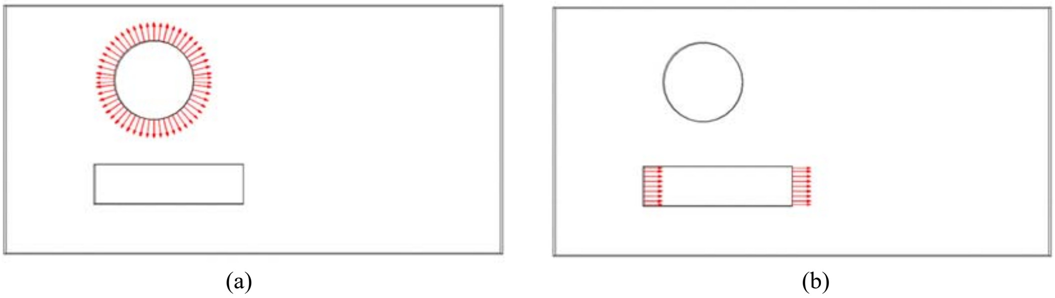
(a) (b)

Fig. 2 Design velocities for parameters shown in Fig. **1**, (a) changing hole diameter, (b) horizontal movement of slot

A number of approaches to calculate design velocity have been proposed in literature [32-34], but are usually restricted to geometric models where the boundary topology remains constant through the parametric perturbation. One of the ways to compute design velocities is by directly differentiating the CAD system using automatic differentiation (AD). Xu et. al. [18] differentiated an in-house CAD tool based on NURBS patches by using the AD tool Tapenade developed by INRIA Sophia-Antipolis [35]. Sanchez et. al. [36] presented the differentiation of another in-house CAD tool by using AD software tool developed at the university of Paderborn [37]. Recently, Mladen et al. [38, 39] demonstrated the differentiation of the open-source CAD system Open-CASCADE (*v7.0*). These approaches to calculate design velocity have significant advantages as they do not require a geometry or mesh to be recomputed. They are both efficient and robust against boundary topology changes. These approaches also avoid the difficulties with numerical accuracy associated with finite difference approaches. The downside is that it requires access to the underlying source code of the CAD system, which is unlikely to become an industrial reality for the major CAD systems in the near future. Further, the derivative calculation for complex geometric configurations and Boolean operations is still challenging.

The calculation of design velocity can be complex for industrial models, where due to the nature of the boundary representation produced by the CAD system, the shape changes caused by a parameter perturbation can be highly constrained, or the model can suffer from robustness issues. The approach used in this work for calculating design velocity is detailed in [22], where the design velocities were calculated for CAD models of industrial complexity, and where the parameters defining the CAD model were used as design variables. The approach is based on the facetted approximations of CAD model geometry generated using open-source mesh generator GMSH [40]. This method is applicable to any feature-based CAD modelling package, places no constraints on changes to boundary topology caused by parametric changes and does not require any special access to the source code of the CAD kernel.

2.2. Adjoint method

In this paper, adjoint sensitivity maps are used to gain insight into how movement of the boundary of the model can impact the objective function. So, the adjoint sensitivity maps suggests the direction that the boundary of the model should be moved, and the relative magnitudes of the movement which should be applied over the boundary, to improve performance. This work contributes no further enhancements to the continuous adjoint method and, thus, a detailed description of the adjoint formulation is omitted. More information about the adjoint development can be found in the literature, e.g. [41]. The adjoint surface sensitivity (ϕ) represents the gradient of objective function with respect to the normal displacement of the surface mesh nodes, and can be mathematically defined as

$$\phi = \frac{dJ}{dX_s}, \tag{2}$$

where J represents the objective function, and δX_s is the movement of surface in the normal direction at a point on the boundary. The computation of adjoint sensitivity requires an additional analysis, where the field adjoint equations are solved. This is done at a computational cost practically independent of the design variables, which is the main advantage of this method, especially where there are a large number of parameters to be considered, such as in this case when working with a CAD model. Using the computed primal and adjoint fields, the adjoint sensitivity map is computed, which shows how the geometry shape should change, in order to achieve a reduction in the objective function. The adjoint surface sensitivity ϕ is provided by the computational analysis package. In this work, the primal analysis is performed with OpenFOAM©, whereas the system of adjoint equations is solved using the Helyx adjoint solver developed by Engys [42].

2.3. Parametric sensitivity and effectiveness

Parametric sensitivity (S) is the change in objective function caused by an infinitesimal perturbation of a CAD parameter. For a computer-aided engineering model, the total change in objective function (dJ) due to parametric perturbation can be predicted as the summation over the boundary of

$$\mathrm{dJ} = -\int_A \phi V_n dA\,, \tag{3}$$

where, ϕ is the surface sensitivity for the objective function, A represents the surface area of the boundary. Knowing the change in objective function due to the parametric perturbation in question, the parametric sensitivity can be calculated by normalizing this value with respect to the size of the perturbation as

$$\mathrm{S} = \frac{\mathrm{d}J}{\mathrm{d}\theta}, \tag{4}$$

where $d\theta$ is the perturbation of a CAD parameter.

Parametric Effectiveness [27] compares the maximum change in performance that can be achieved using the CAD model parameterization, to the maximum performance improvement that can be achieved if the model is not constrained by the parameterization, where both are subjected to the constraint of a unit root-mean-squared boundary movement. The imposed constraint of boundary movement ensures that a parameter moving an area of low sensitivity by a large amount would not be favoured compared to a parameter causing a small localised movement in the areas of high sensitivity. The detailed mathematical derivation of the measure can be found in [27]. The parametric effectiveness can be computed for different combinations of CAD parameters using a single adjoint analysis. This allows the designers to select the appropriate set of parameters to be used for optimization.

Herein, an automated approach is developed to compute the parametric effectiveness of CAD model parameters. In cases where the parametric effectiveness is low, a novel methodology is shown which automatically adds the optimum features to the CAD model feature tree, and thus increases the design freedom of the model. The change in value of parametric effectiveness is used as a criterion to decide which set of the newly inserted features provides the greatest performance improvement or to compare different parameterization options.

3. Methodology for feature insertion

For a CAD model which is determined to have a low parametric effectiveness, this paper describes three approaches to increase its parametric effectiveness through adding new features and associated parameters to the CAD model feature tree. Section 3.1 and 3.2 focus on refining 2D sketches (adding more parameters) on which 3D CAD features are built (e.g. extruded bosses, revolves etc.). Section 3.3 is an enhancement in the definition of the solid feature by adding additional profile sketches to an existing CAD feature.

3.1. Replacing a 2D straight line with a spline

A straight line is a geometric entity with zero curvature, defined only by its start and end points. By contrast, the shape of a spline curve is defined by the position of its control points, which at a minimum must consist of a start and end point, but for which there is no upper limit on the number there can be. Where there are only start and end control points (and no additional tangency information) a spline curve will be equivalent to a straight line between those points. For a sketch, the automated approach described herein will replace all lines in the sketch with spline curves, where the start and end points of the line are used to define the spline, as shown in Fig. 3. If the positions of the start and end points of the spline are not parameterized, then the approach will also add parameters to control their position (a horizontal and vertical parameter). This is implemented for a parametric CAD model constructed in CATIA V5 using the application programming interface (API). It should be noted that replacing a line with a spline controlled by two control points does not increase the flexibility of the model, which comes in the next step.

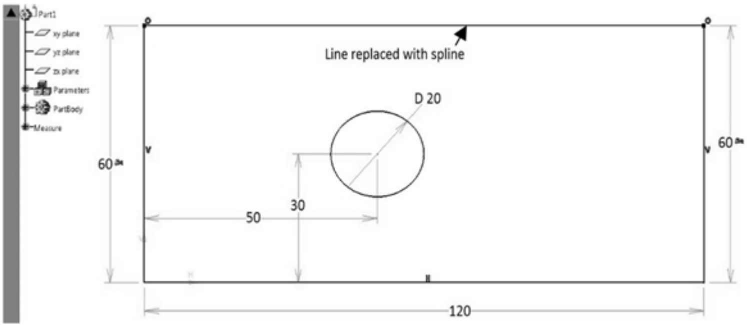

Fig. 3 2D line converted to spline with two control points coincident with end-points of line

3.2. Adding additional control points to 2D spline

Increasing the number of control points defining a spline curve increases the design freedom in the curve and allows it to generate more varied shapes. The next step in the process is to automatically insert additional control points into every spline curve in the sketches. Here, the control points are added at the mid-point of each section of the spline. This means that in the first iteration the control point will be added at t=0.5 along the spline, creating two spline sections. In the next iteration, control points will be added to the midpoint of each spline section (t=0.25 and t=0.75 along the original spline) and so on. Parameters are added to control the values of the *x* and *y* coordinates of the additional control points inserted, as shown in Fig. 4. The insertion of the control points onto the spline curve alone does not change the model shape. However, when the positions of any of the control points are changed during the optimization process, the shape of the spline will update, and any solid modelling feature based upon that sketch will also change in shape accordingly. As such, these new control point parameters have added extra flexibility to the model and perturbing each will generate a design velocity on the model boundary. Now, these design velocities are linked with the adjoint sensitivities to obtain the parametric effectiveness for the addition of each control point. The addition of control points to the model can be repeated many times, and in this work the choice of whether or not to continue adding more control points is based on the improvement in parametric effectiveness they achieve.

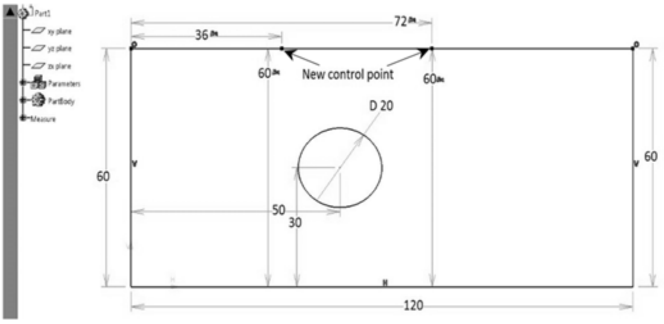

Fig. 4 Additional control points inserted in 2D spline

3.3. Modifying a Multi-Section Solid

Many real-world components vary in profile along their length (e.g. an aircraft wing or an automotive duct). These components are usually modelled in a CAD system by creating sketches at different positions and orientations along the length of the components, and then creating a multi-section solid CAD feature (sometime referred to as a loft) passing through these profiles. Fig. 5 shows a simple multi-section solid feature built in CATIA V5. These features typically pass through the sketches/profiles exactly, but then interpolate the shape of the feature between the sketches. Guide curves are optional curves that run along the length of the multi-section feature, joining the different profiles, and guiding the interpolation that occurs between them.

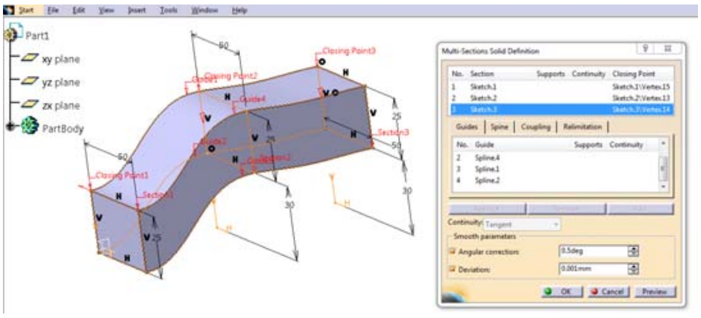

No.	Section	Supports	Continuity	Closing Point
1	Sketch.1			Sketch.1\Vertex.15
2	Sketch.2			Sketch.2\Vertex.13
3	Sketch.3			Sketch.3\Vertex.14

No.	Guide	Supports	Continuity
2	Spline.4		
3	Spline.1		
4	Spline.2		

Continuity: Tangent

Smooth parameters

Angular correction: 0.5deg

Deviation: 0.001mm

Fig. 5 Multi-section solid feature in CATIA V5

Changing the shape of the underlying sketches will change the shape of the resulting feature. One way to update the feature is to use the strategies described in sections 3.1 and 3.2 to update the shapes of the sketches from which it takes its shape. The other way is by inserting additional 2D sketches along the length of the feature, and use the parameters associated with the shape of the new sketch as design variables. The greatest benefit will be obtained from the optimization process if the parameters are added in the areas of high adjoint sensitivities. Once the position to add the sketch is selected (which could be done automatically based on the surface sensitivity, but in this work is done manually), the addition of the new sketches was implemented using the following automated process:

1. Select the multi-section feature (containing region of high adjoint sensitivity) to be updated and define a point on its surface (point with highest adjoint sensitivity) as shown in Fig. 6(a).

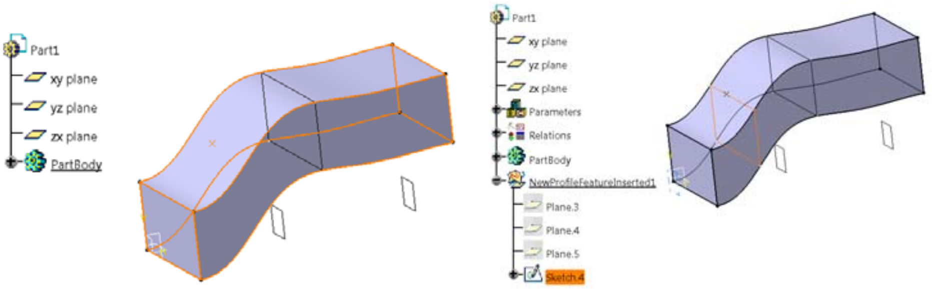

(a) (b)

Fig. 6 (a) A multi-section solid with a point on the surface, (b) Updated multi-section solid with new sketch created passing through the selected point

2. Two planes are created passing through profiles at the start and end of this feature. These two planes are intersected, creating an intersection line. A new plane is created which is coincident to both the computed intersection line and the point of highest sensitivity. In the special case where the planes created at the start and end of the multi-section solid are parallel, then the new plane is created which is parallel to the start plane and is coincident to the selected point.
3. The new plane is intersected with the multi-section feature to get a boundary profile.
4. A sketch is then created on the plane to match the existing profile shape using vertex and edges of the boundary profile as reference.
5. If the selected multi-section feature includes the guide curves, the definition of guides is modified to include the sketch vertex in closest proximity.
6. Finally, the new sketch profile created in step 4 is included in the definition of multi-section feature by recreating the feature to include the old and new profiles as shown in Fig. 6(b).

By following the steps in sections 3.1 to 3.3 any sketch-based features in the model should now be based on sketches controlled by more parameters than before, and any multi-section features should be defined using more sketches than before. The new features and parameters will have been added because they increase the parametric effectiveness of the model. It is important to note that at this stage the shape of the CAD model will not have changed. While the additional features and parameters will add additional control to the model, their current values should be set such that the model shape is the same as the original part. Changing these new control points during the optimisation process will produce design velocities unobtainable with the initial parameter set.

4. Example application: Cantilever Beam

A loaded cantilever beam model is the first test case used to demonstrate a methodology for refining the CAD parameterization during the optimization. The design domain is shown in Fig. 7(a), and the beam is loaded with a traction force at the right-hand edge. Top and bottom segments have been isolated on the left side and are fixed so that they cannot move in the horizontal direction.

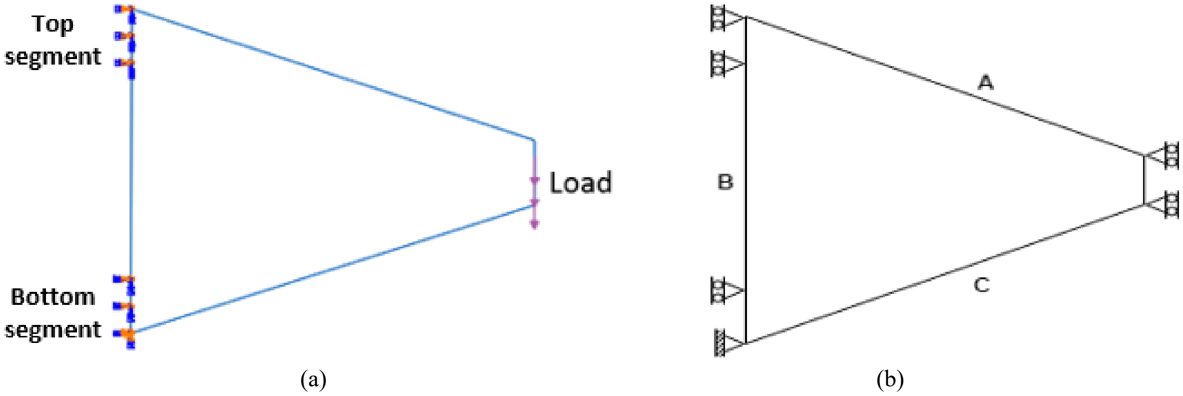

(a) (b)

Fig. 7 (a) Design domain of cantilever beam with boundary conditions, (b) optimization constraints

Fig. 7(b) shows the constraints on the mechanical model. The length of the top and bottom segment of the left edge and the length of right edge are fixed. The bottom left corner of the beam cannot move. Thus, only the sketch lines labelled A, B and C in Fig. 7(b) can be modified during the optimization. The optimization problem considered here is the minimization of strain energy of the system with the constraint that the volume is fixed throughout the optimisation. This can be described as

$$\begin{aligned} \textit{Minimize:} &\quad \textit{strain energy,} \\ \textit{Subject to:} &\quad \textit{change in volume} = 0 \\ \textit{design variables:} &\quad \textit{vector of CAD parameters} \\ \textit{design space:} &\quad \pm 2.5 \times \text{length of left edge of the beam} \end{aligned} \tag{10}$$

The optimization is a compliance minimization problem, therefore the objective function for this test case is to minimize the strain energy. This type of problem is self-adjoint, meaning that a special adjoint solver is not required to compute the surface sensitivities, as the contours of strain energy density on the surface of the model indicate the change in strain energy in the component that can be achieved by moving the boundary. The CAD model is constructed in CATIA V5 as an extruded boss from a sketch of the cross section (Fig. 8). Updating the sketch will therefore update the entire part. The finite-element mesh generation and analysis of the model is done in ABAQUS CAE, which is linked with CAD system and Scipy optimization modules using python scripts. The constraint of constant volume was imposed by defining a parameter (*vol*) in CATIA V5 which returns the volume of the solid as a measurement value. A series of CAD system APIs are developed in this work to automatically obtain the value of *vol* parameter from the CAD system. The computation of gradient of the constraint function is performed by using an API to perturb the CAD parameters by a small amount ($\Delta\theta$) and obtain the new value of the *vol* parameter, and use finite difference method to obtain the gradients as

$$gradient(vol) = \frac{vol^{perturb} - vol^{initial}}{\Delta\theta}. \tag{11}$$

The model was created as an extruded boss feature (pad in CATIA V5). This consisted of designing the cross-section which was extruded to create the beam. The design parameters of the initial model are shown in Fig. 8(a), for which the strain energy contours are shown in Fig. 9(a), and the total strain energy is calculated as 967. The parametric effectiveness computed for the initial model configuration is 0.0 which indicates that the component cannot be optimized without violating the constraints. Now, the parameterisation of the model was updated using the methodology outlined in section-3. Here the approach was used to adaptively refine the model meaning that when new features or parameters were added an optimization step was carried out and terminated before more new features or parameters were added. In all cases the new features and parameters were visible in the CAD model feature tree. The constant volume constraint is used to ensure the model did not grow indefinitely as an optimization with the objective of reducing strain energy will attempt to do. The gradient of this constraint is computed as the change in volume of the beam (computed within CATIA V5) with every parametric update.

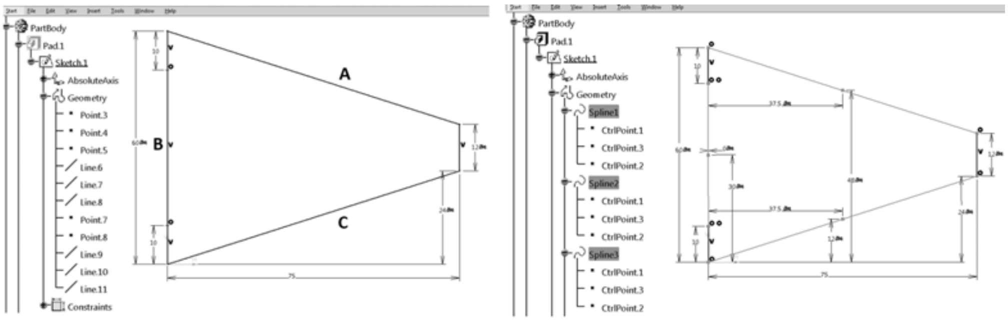

(a) (b)

Fig. 8 (a) CAD 2D sketch with lines, (b) CAD 2D sketch with lines transformed to splines

The refinement of the model was as follows: Firstly the straight lines are transformed to splines each with a control point at its center using the process described in section 3.1 and 3.2 as shown in Fig. 8(b), resulting in a parametric effectiveness to 0.24. The position of new control points is also shown in Fig. 9(b). The model is then optimized using SLSQP algorithm with the constraint of constant volume, resulting in a CAD geometry shown in Fig. 9(c) with effeciveness reduced to 0.16 and a total strain energy of 349 (~ 64 % reduction). Once the optimizer terminates, additional spline control points are automatically added to the splines using a Python CAD system API (shown in Fig. 9(d)) to increase the parametric effectiveness to 0.43.

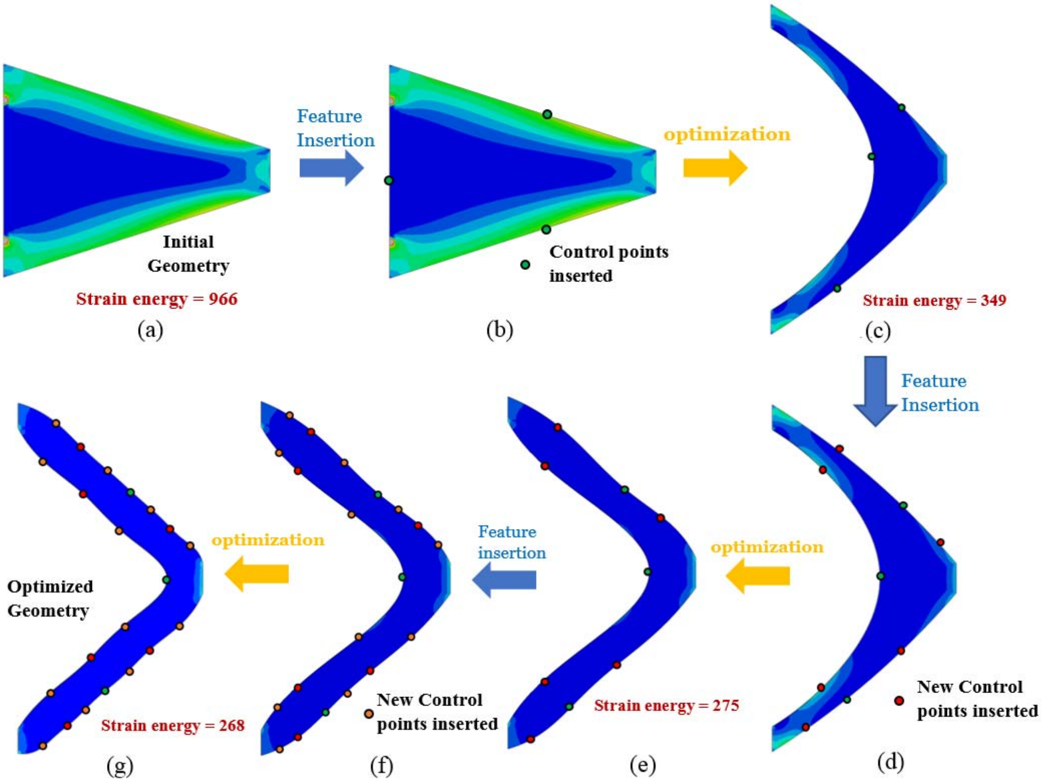

Fig. 9 Adaptively inserting CAD features during optimization

A second stage of optimization was then run with the new set of parameters resulting in the model shown in Fig. 9(e) with the total strain energy of 275 (~ 71.5 % reduction overall) with the parametric effectiveness reduced to 0.15. Now, additional spline control points were added to increase the effectiveness to 0.35 as shown in Fig. 9(f) and a third stage of optimization is performed. At this stage the optimized model (Fig. 9(g)) possessed strain energy of 268 (~ 72.3 % reduction) with an effectiveness of 0.17. Since a very small gain in performance was achieved during the last optimization step, the insertion of new features was stopped at this stage. It is evident that the optimized design is similar to the optimization results obtained in [43, 44]. The process of adding more control points to the spline curve takes less than 5 seconds, while the process of generating the new mesh and running an FEM analysis within ABAQUS takes 25-35 seconds on a 3.60GHz workstation with 16GB RAM. The overall optimization process including the modification of the CAD model and the reduction in strain energy is vizualized in Fig. 9.

5. Example application: S-Bend

The parametric CAD model of the S-Bend duct shown in Fig. 10 was created in CATIA V5. It was modelled using 2D sketch profiles at different positions and orientations, and then by creating a multi-section solid passing through these profiles. The duct is composed of three individual sections i.e. inlet, S-Bend and outlet. The construction of the multi-section solid feature uses guide curves to control the orientation and curvature of the outer boundary, particularly for the S-Bend area. As the inlet and outlet ducts join with other components their shape is fixed and they are not considered for optimization. This means that the only geometrical features that can be varied are the two sketches (sketch 1 and sketch 2) describing the profile of the S-Bend at different positions along its length.

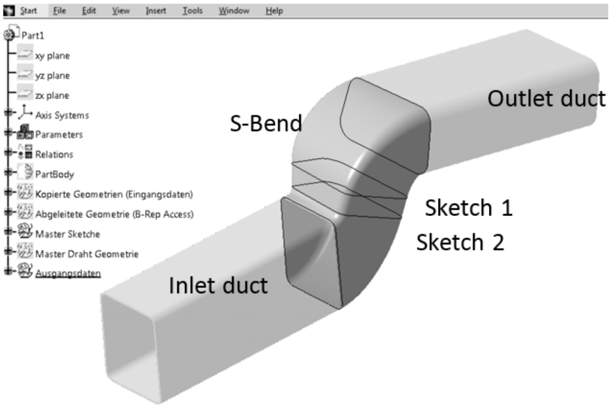

Fig. 10 CAD model of S-Bend duct created in CATIA V5

The two sketches are parameterized using the parameters as shown in Fig. 11, while the orientation of the sketch planes is defined by an angle parameter relative to the inlet plane. The fluid domain used for CFD analysis is extracted from the body within the CAD environment, by joining the face patches with tangency constraints. This imposes C_1 continuity between the wall faces.

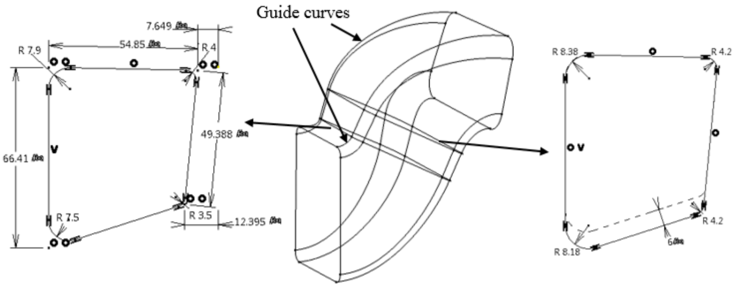

Fig. 11 S-Bend CAD parameterization

The flow is laminar, with Reynolds number $R_e = 350$, calculated with a hydraulic diameter of $D_h = 0.053m$, inlet velocity $u = 0.1m/s$, and kinematic viscosity $v = 1.511\ X\ 10^{-5}\ m^2/s$. The CFD mesh created in ICEM CFD [45] comprises 486,000 elements and is shown in Fig. 12. The results of flow analysis are shown in Fig. 13, where the pressure and velocity contours are plotted along with streamlines.

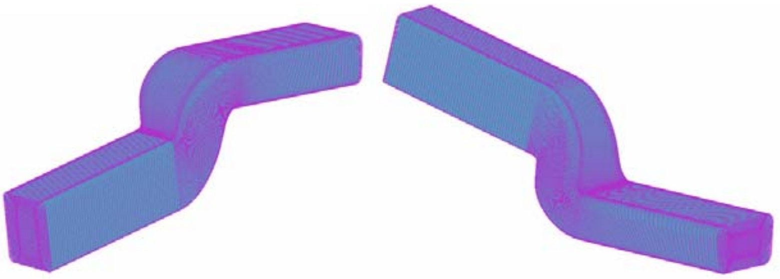

Fig. 12 CFD analysis mesh for S-Bend

The objective function considered for optimization is the power dissipation through the duct [24], defined as

$$J = \int_A v \cdot \hat{n} \left(p + \frac{1}{2} v^2 \right) dA\,, \tag{12}$$

where p and v are the pressure and velocity of the flow, and A and $\hat{n}$ are the surface area of the duct and the unit normal of the duct pointing away from the fluid area.

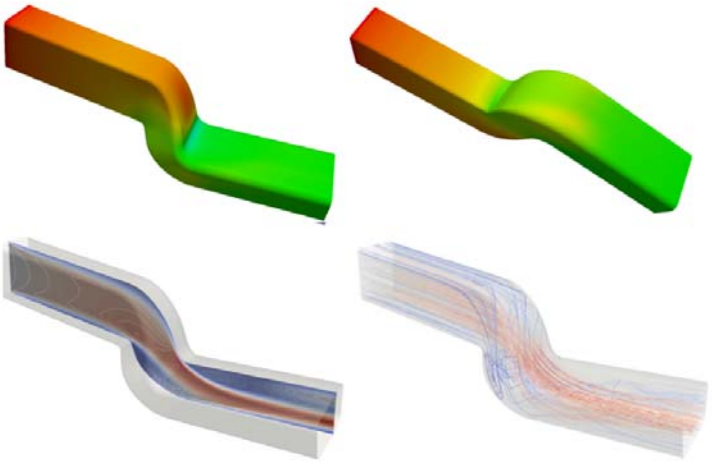

Fig. 13 Pressure contours (top) and velocity contours and streamlines (bottom) computed for the base geometry

In this example, the adjoint was computed as a separate analysis step using Helyx [42]. The adjoint sensitivities of the objective function with respect to the normal displacement of the surface are computed at the first optimization cycle and presented in Fig. 14. High sensitivities can be seen at the areas of the duct with high curvature. These are the areas in Fig. 14, where flow separation occurs, contributing to an increase in power dissipation. The adjoint sensitivities indicate the geometry displacement that would control the flow recirculation and reduce the objective function. It is clear though, the changes suggested by the adjoint sensitivities are local and cannot be implemented easily by the original design parameters (Fig. 11). The value of parametric effectiveness calculated for the initial configuration is 0.14, which is taken here as an indication of the need to add new features to the model before optimization. Again, this is achieved automatically following the methodology described in section-3.

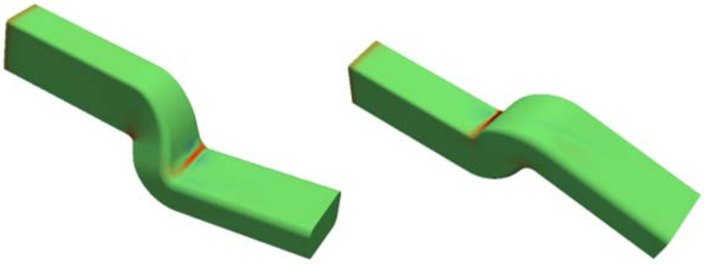

Fig. 14 Adjoint sensitivities contour. To minimize the objective function (dissipated power) the surface should be pulled out at positive values (warm colours) or pushed in (cold colours).

5.1. Replacing 2D lines with splines with added flexibility

The first step to increase the design flexibility of the S-Bend model is to replace straight lines in existing sketches and parameterizing the positions of the end points. Fig. 15 shows that the straight lines in the two sketch profiles (initially parameterized as shown in Fig. 11) are converted to spline curves and spline control points have been added at the centre of each spline curve. In this case, the radius of circular arcs (defining the rounded corners) and their tangent with the lines are formulated as constraints. A total of eight design parameters are used (in addition to the radii of corner circles and tangency between lines and circles) to make the sketch fully constrained. This results in a total of 32 parameters with a parametric effectiveness of 0.22.

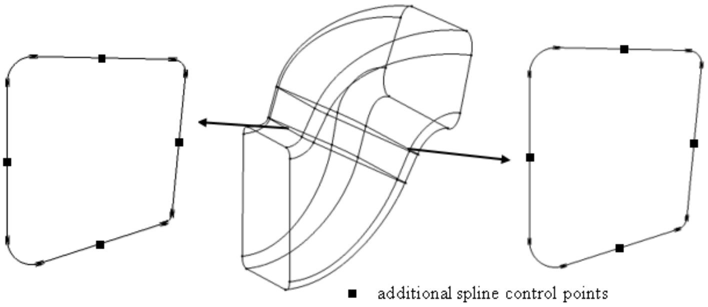

Fig. 15 Replacing lines with splines with additional control points

5.2. Addition of multiple cross-section sketches

Since the duct is defined as a multi-section solid, the process described in section 3.3 was used to insert new 2D sketch profiles along the length of the duct, and the parameters associated with new sketches used as design variables. It is apparent that the best location to add sketches would be in the areas of high adjoint sensitivity, increasing the design flexibility in these areas. Analysing the adjoint sensitivity map in Fig. 14, the two multi-section features defining the two bend areas of the duct are user selected as a point on the surface of each feature in the region of high adjoint sensitivity. The new sketch profile **A** and **D** are inserted using the automated process described in section 3.3 and are shown in Fig. 16. The addition of sketch-A resulted in an increase in parametric effectiveness to 0.57, and then adding sketch-D increased the effectiveness to 0.61 (total number of parameters increased to 48). Further, using the methodology of section 5.1 to convert the straight lines of new sketches to spline curves with additional control points resulted in a very small increase in the parametric effectiveness, and thus it was decided that with a parametric effectiveness of 0.61, the optimization should be attempted.

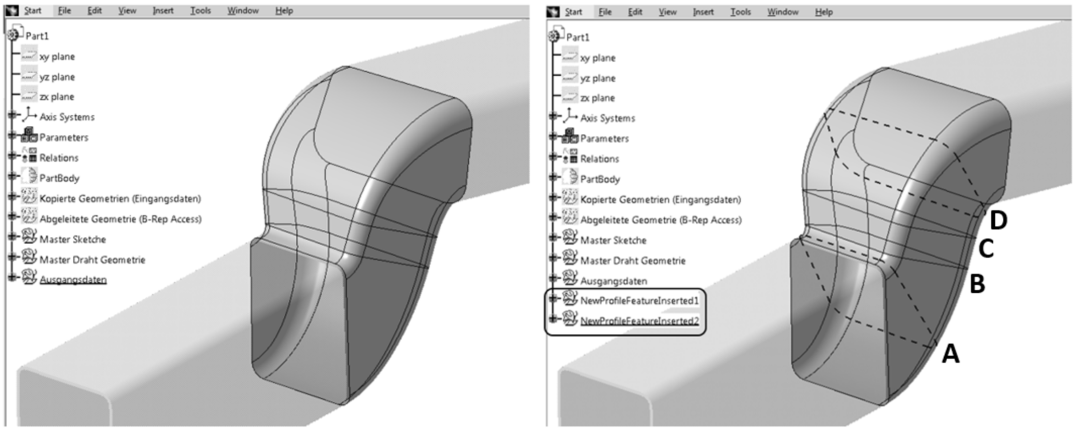

(a) (b)

Fig. 16 Insertion of new cross-section sketches in the CAD feature tree (a) original CAD, (b) CAD model with new sketches shown with broken lines.

5.3. Optimization with new parameters/features

The effect of the increased value of parametric effectiveness is demonstrated using the design velocity contours comparing the movement of the CAD model using the steepest decent boundary movement based on the initial parameterization (selected by designer), with the steepest decent boundary movement of the parameterization created by inserting features into the CAD model to get the maximum parametric effectiveness. It can be seen in the design velocity contours in Fig. 17(b) how the new features allow the movement of CAD model boundary in the areas close to the optimum movement suggested by the contours of the adjoint sensitivity map in Fig. 14, compared to Fig. 17(a) which shows much less movement localised in the highly sensitive region given by the original parameters.

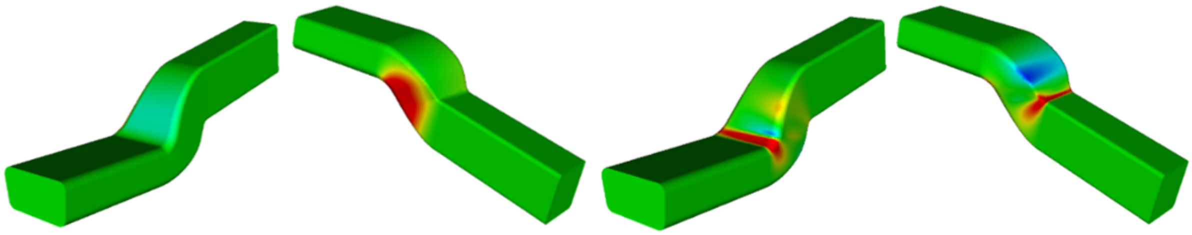

(a) (b)

Fig. 17 Design velocity contours (red as positive and blue as negative) for the overall boundary movement $\boldsymbol{dV = 1\,E^{-4}}$, (a) initial parameters, (b) with feature insertion

In this work, the optimization was performed using different parameterizations. The first was the one selected by the designers, and the others were created by inserting new features into the CAD model feature tree using the described approach. The insertion of new features was done in three different ways: (1) adaptive parameterization where each time a new feature is added to the model and an optimization was carried out before additional features are added, (2) progressive parameterization where it was determined up front that new features should be added to the model after fixed number of optimization steps, and (3) static parameterization, where as many new features were added to the model before the start of optimization as were required to improve the Parametric Effectiveness as much as possible. The results of optimization with an objective of minimizing power-loss performed using different methodologies are shown in Fig. 18. A gradient-based optimization method (steepest decent) is employed to minimize the objective function using the CAD parameters as design variables. With each optimization step, the CAD parameter values are updated using a CAD system API developed during this work and for each step a new analysis mesh was created.

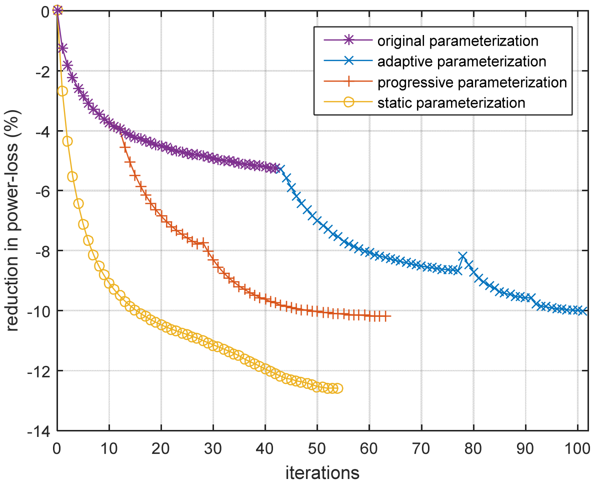

Fig. 18 Optimization with CAD features inserted in S-Bend (power-loss as objective function)

The objective function was reduced by 5.25% in 42 steps when optimized using the initial set of design parameters. Following the adaptive and progressive parameterization strategy, the objective function was reduced by 10% in 102 and 63 optimization steps respectively. Using the static parameterization strategy, the maximum reduction in objective function was 12.6% and required only 54 steps. The computational cost for the optimization processes is outlined in Table 1.

Table 1 Time taken by the optimization process

optimization	Time (approx..)
original parameters	14 hrs
adaptive parameterization	22 hrs
progressive parameterization	29 hrs
static parameterization	19 hrs

Jesudasan et al. [21] presented an adaptive parameterization strategy, and showed that higher reduction in objective function can be achieved by adaptively refining the NURBS patch using knot insertion during the optimization. In this work, it was found that refining the CAD model parameterization at the start of optimization (static parameterisation) was superior to the other re-parameterization approaches in terms of optimization time and improvement in performance achieved. In the remaining paper, the optimization results are shown for the static parameterization. The evolution of parametric effectiveness during the optimization process is shown in Fig. 19. The parametric effectiveness tends to a small value as the geometry reaches its optimum shape. This is because the parameters have become less able to improve performance as they tend to their optimum value.

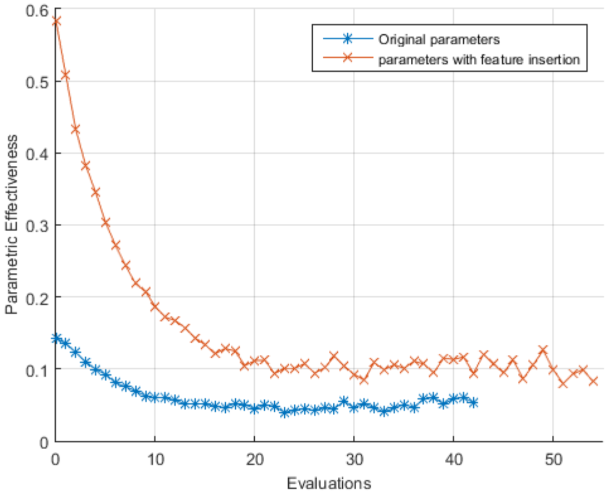

Fig. 19 Evolution of Parametric effectiveness during the optimization

The comparison between the initial and optimized CAD model is shown in Fig. 20. The optimized design shows some ripples in the shape near the regions where the S-Bend section of the duct meets the fixed inlet and outlet. On comparing the adjoint sensitivities for the initial (shown in Fig. 14) and the optimized geometry (shown in Fig. 21), it can be seen that the optimization process has significantly reduced the adjoint sensitivities in the bend regions (which were initially highly sensitive), leading to an optimized design which is close to optimum.

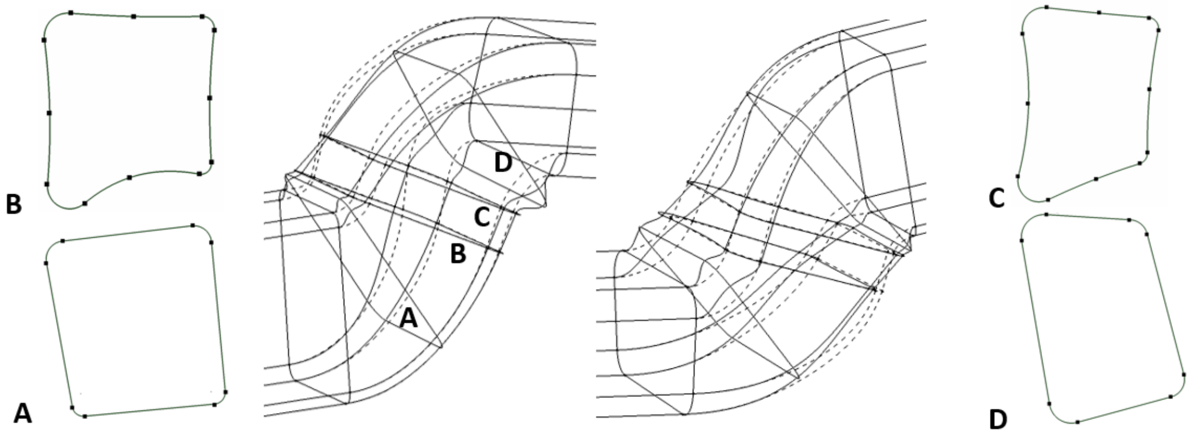

Fig. 20 Comparison between original (broken lines) and optimized (solid line) CAD model for the geometry optimized using feature insertion methodology (middle images from opposite orientations).

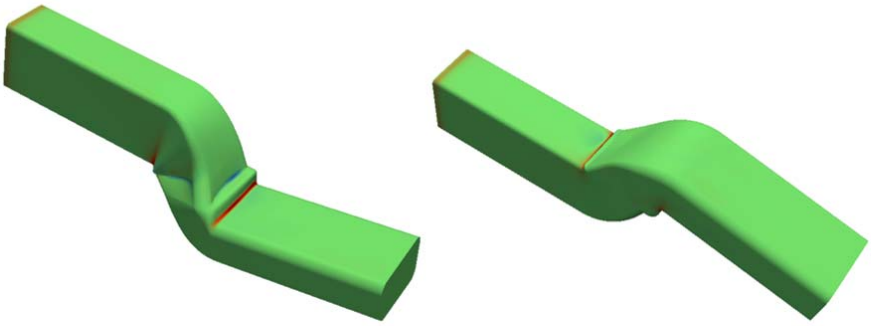

Fig. 21 Adjoint sensitivities contour on the optimized geometry

The flow streamlines for the initial and optimized geometries are shown in Fig. 22. It can be seen that the initial flow field possess greater non-uniformity compared to the optimized flow. The adjoint sensitivities suggested a surface movement that would reduce the high adverse pressure gradients observed on the high-curvature areas of the S-Bend. As the result of optimization, the flow requires less energy to remain attached, subsequently reducing the recirculation region, and thus reduces the objective function. This is seen in Fig. 23, where the contours of velocity magnitude are plotted at different cross-sections along the duct.

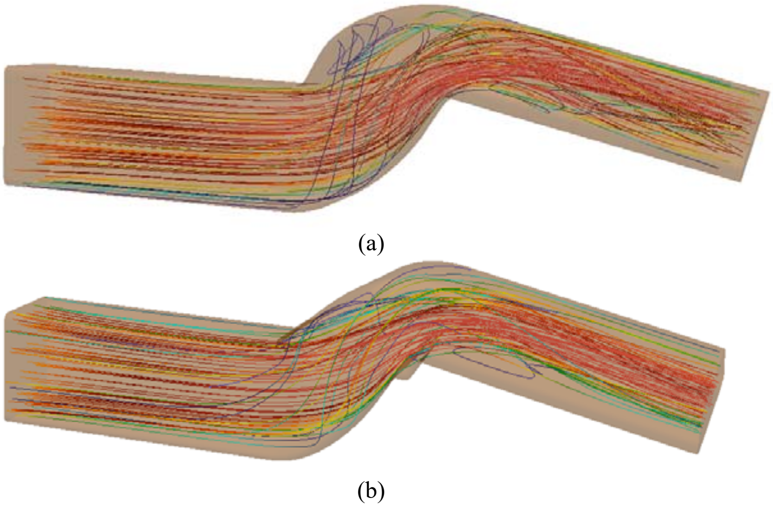

(a)

(b)

Fig. 22 Flow streamlines for (a) initial and (b) optimized geometry

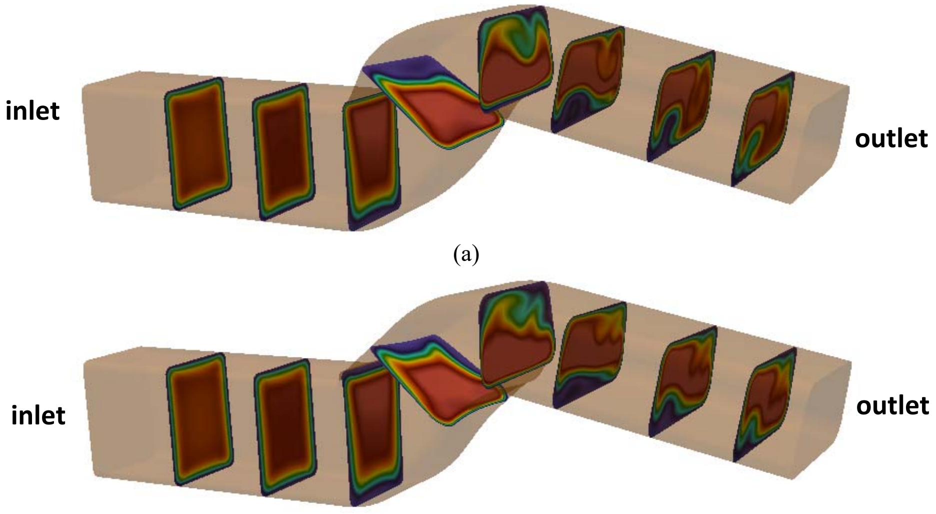

(a)

(b)

Fig. 23 Contour plots of velocity magnitude for the (a) initial and (b) optimized geometry

6. Discussion

In this work, a process has been described where the parameterization of a CAD model has been modified automatically using the python APIs to the CAD system. This provides the opportunity to achieve a better optimum. The approaches used were to: i) replace line entities in a sketch with spline curves, ii) to increase the number of control points used to define a spline, thereby providing additional shape flexibility compared to the line entities they replaced and iii) to insert new sketch profiles along a multi-section solid such that there is more control over the shape of a body along its length. The first two will be beneficial to all sketch-based features in a CAD system (e.g. boss, revolution etc.). Adjoint surface sensitivities have been used to predict the effect of adding features, since this allows the effect of many different shape changes to be evaluated using a single analysis. The metric for determining whether a new feature was needed was parametric effectiveness, where a low value indicated a need for improvement. The approach outlined may sometimes result in the features getting inserted where parameters already exist, or where more design flexibility is not required. But these situations can be identified by a decrease in the value of parametric effectiveness when such features are inserted. This happens because as increasing number of parameters are moving the same region of the boundary, or are moving less sensitive regions, the parameterization will be penalised by the unit root mean squared constraint inherited in the calculation of parametric effectiveness. The process has been implemented such that the current state of a model is saved before new features are added. Should adding the new features or parameters not improve the parametric effectiveness then the process will revert to the previous model.

The Python Scipy [29] optimization framework used in this work was coupled with the developed tools such that it automatically inserts new CAD features at the start of optimization or during the optimization. One of the difficulties in automated shape optimization using CAD is to establish an appropriate lower- and upper-bounds of the design variables. This is usually required to ensure the robustness of the process such that the CAD model boundary topology does not change, and that the model can regenerate. The approach that is used in this work is robust against boundary topology changes. To ensure the robustness of the CAD model update, the CAD system API is used to perturb each parameter by a fixed amount ($\pm B_{max}$) and ensures the CAD model is updated successfully. If the model fails to update, then the perturbation size is reduced by 10% and reattempted until the model successfully regenerates. The resulting perturbation is used to compute sensitivities for that parameter. The same process is used for the newly inserted control points.

For the beam model, as the finite element mesh generation and analysis were not very expensive (in the order of seconds). The insertion of new CAD features was done using an iterative approach, where new features were added once the optimisation was complete for the current set. In section 5, where computationally expensive CFD runs were performed during the optimization, an iterative approach for generating feature-based CAD models using feedback from CFD simulations [27] became prohibitive. So, the proposed approach is to use the techniques described in this paper to refine the CAD parameterization up front, and then optimising the model. The comparison of optimization results for power-loss across the duct for initial parameters and the ones obtained using the automatic parameterization scheme for feature insertion are shown in Fig. 18, where it can be seen that the CAD model with highest parametric effectiveness resulted in comparatively higher reduction in objective function compared to the ones with lower parametric effectiveness. Also, it was interesting to find that the optimization using different strategies converged to different local minima, and the static parameterization strategy with new features inserted at the start of optimization resulted in better optimized geometry compared to the optimums reached when insertion of features was done during the optimization. Further, analysing the computational time required for the two optimization processes in Table 1, it was found that the optimization process with newly added features took more time compared to the optimization using the original parameters. This increased computational time resulted from the increase in number of iterations taken by the optimizer for convergence. Although, new features resulted in more than 7% reduction in power-loss compared to that achieved with the original parameters, there is the potential for the computational cost to become a limiting factor. In such cases, either the optimizer should be limited by the maximum number of CFD runs, or other optimization methods with higher-order of convergence can be employed, which is an interesting area for further research.

7. Conclusion

Through this work it has been shown that:

- Automated python scripts have been developed to automatically insert CAD features for modifying 2D sketches and multi-section solids built in CATIA V5.
- The parametric effectiveness of inserting new features to the original CAD model can be calculated using a single adjoint analysis. This can then be used as a criterion to select the optimum feature to be inserted, which would result in better optimization.
- The additional shape flexibility imparted to the model by updating the parameterization, leads to a better optimised component than would have been possible using the original parameters alone.
- The increased performance as a result of the optimization must be contrasted with the increased runtime.

Acknowledgement

This work has been conducted within the IODA project (http://ioda.sems.qmul.ac.uk), funded by the European Union HORIZON 2020 Framework Programme for Research and Innovation under Grant Agreement No. 642959. Authors gratefully acknowledge the discussions with Dr. Carsten Othmer on the optimization results presented in section 5.

References

1. Samareh J (2001) Survey of shape parametrisation techniques for high-fidelity multidisciplinary shape optimization. AIAA J 39:877-884. doi: https://doi.org/10.2514/2.1391

2. Belegundu A, Rajan S (1988) A shape optimization approach based on natural design variables and shape functions. Comput.Methods Appl.Mech.Eng. 66:87-106. doi: https://doi.org/10.1016/0045-7825(88)90061-8

3. Jameson A, Martinelli L, Pierce N (1998) Optimum aerodynamic design using the Navier–Stokes equations. Theor. Comput. Fluid Dyn. 10:213-237. doi: https://doi.org/10.1007/s001620050060

4. Helgason E, Krajnovic S (2012) Aerodynamic shape optimization of a pipe using the adjoint method. In: ASME International Mechanical Engineering Congress & Exposition, 7: 9-15.https://doi.org/10.1115/IMECE2012-89396

5. Jameson A (2004) Efficient aerodynamic shape optimization. AIAA paper 4369:2004.

6. Samareh J (2004) Aerodynamic shape optimization based on free-form deformation. In: 10th AIAA Multidisciplinary analysis and optimization conferencehttps://doi.org/10.2514/6.2004-4630

7. Kenway GK, Kennedy GJ, Martins J (2010) A CAD-free approach to high-fidelity aerostructural optimization. In: 13th AIAA/ISSMO Multidisciplinary Analysis Optimization Conferencehttps://doi.org/10.2514/6.2010-9231

8. Hoogervorst JEK, Elham A (2016) Wing aerostructural optimization using the individual discipline feasible architecture. In: 17th AIAA/ISSMO multidisciplinary analysis and optimization conference: 3996.https://doi.org/10.1016/j.ast.2017.02.012

9. Sederberg TW, Parry SR (1986) Free-form deformation of solid geometric models. In: 13th annual conference on computer graphics and interactive techniques 20: 151-160.

10. Anderson CW, Crawford-Hines S (2000) Fast generation of nurbs surfaces from polygonal mesh models of human anatomy. Colorado State University Computer Science Technical Report CS-99 101

11. Guo B (1997) Surface reconstruction: from points to splines. Comput.-Aided Des. 29:269-277. doi: https://doi.org/10.1016/S0010-4485(96)00055-3

12. CATIA V5. http://www.3ds.com/products-services/catia/. Accessed 01/27/2017

13. Shah JJ (1991) Assessment of features technology. Comput.-Aided Des. 23:331-343. doi: https://doi.org/10.1016/0010-4485(91)90027-T

14. Latif M, Boyd R, Hannam R (1993) Integrating CAD and manufacturing intelligence through features and objects. International Journal of Computer Integrated Manufacturing 6:87-93. doi: https://doi.org/10.1080/09511929308944558

15. Salomons OW, van Houten FJ, Kals H (1993) Review of research in feature-based design. Journal of Manufacturing Systems 12:113-132. doi: https://doi.org/10.1016/0278-6125(93)90012-I
16. Martin MJ, Andrés E, Widhalm M, Bitrián P, Lozano C (2012) Non-uniform rational B-splines-based aerodynamic shape design optimization with the DLR TAU code. Proceedings of the Institution of Mechanical Engineers, Part G: Journal of Aerospace Engineering 226:1225-1242. doi: https://doi.org/10.1177%2F0954410011421704
17. Yu G, Müller J, Jones D (2011) CAD based shape optimization using adjoint sensitivities. Comput Fluids 46:512-516. doi: https://doi.org/10.1016/j.compfluid.2011.01.043
18. Xu S, Jahn W, Müller J (2014) CAD based shape optimization with CFD using a discrete adjoint. Int J Numer methods Fluids 74:153-168. doi: https://doi.org/10.1002/fld.3844
19. Burgos MJ (2015) NURBS-Based Geometry Parameterization for Aerodynamic Shape Optimization. Dissertation, PhD thesis, Universidad Politecnica de Madrid
20. Xu S, Timme S, Mykhaskiv O, Müller J (2017) Wing-body junction optimisation with CAD-based parametrisation including a moving intersection. Aerospace Science and Technology 68:543-551. doi: https://doi.org/10.1016/j.ast.2017.06.014
21. Jesudasan R, Zhang X, Müller J (2017) Adjoint optimisation of internal turbine cooling channel using NURBS-based automatic and adaptive parametrisation method. In: ASME Gas Turbine Conference, GTIndia2017-4669
22. Agarwal D, Robinson TT, Armstrong CG, Marques S, Vasilopoulos I, Meyer M (2018) Parametric design velocity computation for CAD-based design optimization using adjoint methods. Engineering with Computers 34:225-239. doi: http://dx.doi.org/10.1007/s00366-017-0534-x
23. Giles MB, Pierce N (2000) An introduction to the adjoint approach to design. Flow Turbul Combust 65:393-415. doi: https://doi.org/10.1023/A:1011430410075
24. Othmer C (2008) A continuous adjoint formulation for the computation of topological and surface sensitivities of ducted flows. Int J Numer Methods Fluids 58:861-877. doi: https://doi.org/10.1002/fld.1770
25. Mader CA, RA Martins J, Alonso JJ, Der Weide EV (2008) Adjoint: an approach for the rapid development of discrete adjoint solvers. AIAA J 46:863-873. doi: https://doi.org/10.2514/1.29123
26. Nadarajah S, Jameson A (2001) Studies of the continuous and discrete adjoint approaches to viscous automatic aerodynamic shape optimization. In: 15th AIAA Computational Fluid Dynamics Conference: 2530.https://doi.org/10.2514/6.2001-2530
27. Robinson TT, Armstrong CG, Chua HS (2013) Determining the parametric effectiveness of a CAD model. Engineering with Computers 29:111-126. doi: https://doi.org/10.1007/s00366-011-0248-4
28. Robinson TT, Armstrong CG, Chua HS (2012) Strategies for adding features to CAD models in order to optimize performance. Structural and Multidisciplinary optimization 46:415-424. doi: https://doi.org/10.1007/s00158-012-0770-z
29. Scipy Optimize. https://docs.scipy.org/doc/scipy/reference/optimize.html. Accessed 01/27/2017
30. Python 3.5. http://www.python.org/downloads/release/python-350/. Accessed 10/05/2017
31. Hammond M., Robinson A (2000) Python programming on win32: Help for windows programmers. O'Reilly Media Inc.,
32. Kripac J (1995) A mechanism for persistently naming topological entities in history based parametric solid models. In: Proceedings of the 3rd ACM symposium on solid modelling and applications: 21-30.
33. Chen S, Torterelli D (1997) Three-dimensional shape optimization with variational geometry. Structural Optimization 13:81-94. doi: https://doi.org/10.1007/BF01199226
34. Hardee E, Chang K, Tu J, Choi KK, Grindeanu I, Yu X (1999) A CAD-based design parameterization for shape optimization of elastic solids. Adv Eng Softw 30:185-199. doi: https://doi.org/10.1016/S0965-9978(98)00065-9
35. TAPENADE. https://www-sop.inria.fr/tropics/tapenade.html. Accessed 02/21/2018
36. Torreguitart IS, Verstraete T, Mueller L (2017) Optimization Of The Ls89 Axial Turbine Profile Using A Cad And Adjoint Based Approach. In: 12 th European Conference on Turbomachinery Fluid dynamics & Thermodynamics
37. Walther A, Griewank A (2010) A Package for the Automatic Differentiation of Algorithms Written in C/C. URL https://projects.coin-or.org/ADOL-C
38. Banovic M, Mykhaskiv O, Auriemma S, Legrand H, Walther A, Müller J (2017) Automatic Differentiation of the Open CASCADE Technology CAD System and its coupling with an Adjoint CFD. Optimization Methods & Software. doi: http://www.optimization-online.org/DB_HTML/2017/03/5931.html
39. Auriemma S, Banovic M, Mykhaskiv O, Legrand H, Müller J, Walther A (2016) Optimisation of a U-bend using CAD-based adjoint method with differentiated CAD kernel. In: ECCOMAS Congress
40. Geuzaine C, Remacle JF (2009) GMSH: A three-dimensional finite element mesh generator with built-in pre- and post-processing facilities. Int J Numer methods Eng 79:1309-1331. doi: https://doi.org/10.1002/nme.2579

41. Papoutsis-Kiachagias E, Giannakoglou KC (2016) Continuous adjoint methods for turbulent flows, applied to shape and topology optimization: industrial applications. Archives of Computational Methods in Engineering 23:255-299. doi: https://doi.org/10.1007/s11831-014-9141-9

42. Karpouzas GK, Papoutsis-Kiachagias EM, Schumacher T, Villiers Ed, Giannakoglou KC, Othmer C (2016) Adjoint optimization for vehicle external aerodynamics. International Journal of Automotive Engineering 7:1-7. doi: https://doi.org/10.20485/jsaeijae.7.1_1

43. Mei Y, Wang X, Cheng G (2008) A feature-based topological optimization for structure design. Advances in Engineering Software 39:71-87. doi: http://dx.doi.org/10.1016/j.advengsoft.2007.01.023

44. Wang MY, Wang X, Guo D (2003) A level set method for structural topology optimization. Computer Methods in Applied Mechanics and Engineering 192:227-246. doi: http://dx.doi.org/10.1016/S0045-7825(02)00559-5

45. Ansys ICEM CFD. http://www.ansys.com/en-GB/Services/training-center/platform/introduction-to-ansys-icem-cfd-Hexa. Accessed 09/27/2017